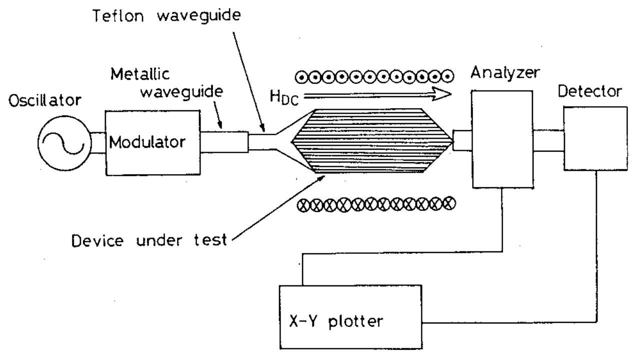

Fig. 5. Setup for measurement of polarized direction.

the mode conversion is degraded only 0.04 percent at 49 GHz, when the applied magnetic field is 1500 (Oe). So far as conductor loss is concerned, insertion loss of less than 1 dB is expected for the device length of 5 cm.

III. Experimental Examination

In order to confirm experimentally our idea, we fabricated an artificial anisotropic waveguide and performed experiments on mode conversion. The fabricated waveguide consists of a YIG polycrystalline slab of 0.72-mm thickness loaded by copper strips, which are formed by etching the vacuum-evaporated copper thin film. The width and periodicity of strips are 1.2 mm and 2.0 mm, respectively. The artificial anisotropic waveguide is 5.0 cm long.

The guiding wave was launched from a metallic waveguide by way of a teflon waveguide and detected through the analyzer (Fig. 5). As is mentioned in the previous section, when the two cross-polarized modes are phase matched, nonreciprocal mode conversion occurs by virtue of magnetic anisotropy which is produced by applying a dc magnetic field parallel to the propagation direction in the YIG waveguide. This phenomenon is observed as the rotation of polarized direction (Fig. 6). In Fig. 6, the abscissa and ordinate indicate the angle of the analyzer and the detected power, respectively. Here, the polarized direction is defined as the direction making a right angle to the direction where the detected power is minimum. It is observed that the polarized direction rotates about 40 (degrees) when the applied field is 300 (Oe). On the other hand, it rotates in the reverse direction when the applied field is reversed. This means that nonreciprocal mode conversion occurred in the fabricated waveguide, as the reversal of the applied magnetic field is equivalent to that of propagation direction. Though the waveguide was designed to be phase matched at 49 GHz, the maximum mode conversion was obtained at 52 GHz. We attribute this to the fabrication errors.

We performed the same experiment on the YIG slab of the same dimension without copper strips. In this case, no mode conversion could be observed. This implies that phase matching was not taken in the YIG slab without copper strips.

It has been shown by the experimental results that the conductor strips properly placed on the dielectric slab cause phase matching between the cross-polarized modes.

IV. Conclusions

Phase matching by the use of an artificial anisotropic structure and its application to a mode converter are proposed for millimeter-wave dielectric circuitry. Phase-matched dielectric planar waveguide is designed by using a rigorous analysis. Mode conversion characteristics are also studied in the artificial anisotropic waveguide composed of a magnetic anisotropic material. Nonreciprocal mode conversion is observed in the YIG artificial anisotropic waveguide. The polarized direction rotates about 40 (degrees) when the magnetic field of 300 (Oe) is applied to the waveguide of 5.0-cm length. Therefore, it is concluded that the planar mode converter and/or isolator can be constructed in the artificial anisotropic waveguide by virtue of magnetic anisotropy.

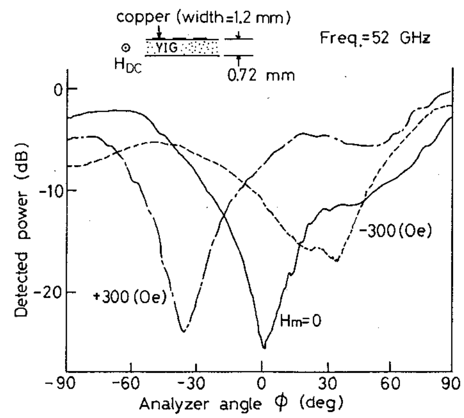

Fig. 6. Observed rotation of polarized direction.

References

[1] G. M. Lindgren, "Coupler design in open dielectric waveguide with web registration," in *IEEE Int. Microwave Symp. Dig.*, 1981, pp. 11–13.
[2] G. L. Matthaei, D. C. Park, Y. M. Kim, and D. L. Johnson, "Some dielectric-waveguide filter structure," in *IEEE Int. Microwave Symp. Dig.*, 1983, pp. 299–301.
[3] M. Muraguchi, K. Araki, and Y. Naito, "A new type of isolator for millimeter-wave integrated circuits using a nonreciprocal travelling-wave resonator," *IEEE Trans. Microwave Theory Tech.*, vol. MTT-30, pp. 1867–1873, Nov. 1982.
[4] S. Wang, M. Shah, and J. D. Crow, "Studies of the use of gyrotropic and anisotropic materials for mode conversion in thin-film optical-waveguide applications," *J. Appl. Phys.*, vol. 43, pp. 1861–1875, Apr. 1972.
[5] J. Warner, "Nonreciprocal magnetooptic waveguide," *IEEE Trans. Microwave Theory Tech.*, vol. MTT-23, pp. 70–78, Jan. 1975.
[6] T. Mizumoto and Y. Naito, "Phase matched optical dielectric waveguide using the artificial anisotropic structure," *Electron. Commun. in Japan*, vol. 66, pp. 117–125, May 1983.
[7] E. Yamashita and K. Atsuki, "Analysis of microstrip-like transmission lines by nonuniform discretization of integral equations," *IEEE Trans. Microwave Theory Tech.*, vol. MTT-24, pp. 195–200, Apr. 1976.
[8] S. Yamamoto, Y. Koyamada, and T. Makimoto, "Normal-mode analysis of anisotropic and gyrotropic thin-film waveguides for integrated optics," *J. Appl. Phys.*, vol. 43, pp. 5090–5097, Dec. 1972.
[9] D. Mirshekar-Syahkal and J. B. Davies, "Accurate solution of microstrip and coplanar structures for dispersion and for dielectric and conductor losses," *IEEE Trans. Microwave Theory Tech.*, vol. MTT-27, pp. 694–699, July 1979.

A Design Method of Bandpass Filters Using Dielectric-Filled Coaxial Resonators

MORIKAZU SAGAWA, MITSUO MAKIMOTO, AND SADAHIKO YAMASHITA, MEMBER, IEEE

Abstract —**Design formulas for capacitively coupled bandpass filters using dielectric-filled coaxial resonators are derived and experimentally verified. The most important advantage of this filter is its ability to provide**

Manuscript received June 14, 1984; revised September 12, 1984.
The authors are with Matsushita Research Institute Tokyo, Inc., Higashimita, Tama-Ku, Kawasaki 214, Japan.

0018-9480/85/0002-0152$01.00 ©1985 IEEE

wide stopband characteristics for harmonics suppression. Its features can be obtained from the configuration using both quarter-wavelength uniform impedance resonators (UIR's) and stepped impedance resonators (SIR's).

I. Introduction

The miniaturization of radio communication equipment is in progress with the development of mobile communications. This technological trend requires compact bandpass filters; besides, output filters of nonlinear circuits, such as oscillators and amplifiers, must have the ability to provide wide stopband characteristics for harmonics suppression. The use of conventional quarter-wavelength uniform impedance resonators (UIR's) for output filters is usually not appropriate because of their poor harmonics suppression.

As one of the approaches to overcome this problem, the authors previously introduced the use of the stepped impedance resonator (SIR) as a filter element [1]–[3].

This paper describes the SIR filled with high-Q dielectric material and its application to bandpass filters with wide stopband characteristics.

Firstly, fundamental parameters such as resonance properties, unloaded-Q, and slope parameters of the SIR were analytically derived. Secondly, the design formulas for capacitively coupled bandpass filters were derived from the admittance inverter parameters. Thirdly, the method of spurious suppression for wide stopband characteristics was considered. Finally, an experimental bandpass filter was designed and fabricated, based on these design formulas and in consideration of spurious suppression. The experimental performance data should be in close agreement with the design results.

II. Dielectric-Filled Stepped Impedance Resonator

A. Resonance Properties of the SIR

The resonator structure of a dielectric-filled SIR is shown in Fig. 1. Fig. 1(a) shows an inner conductor step-shaped structure (type (A)) and Fig. 1(b) shows an outer conductor step-shaped structure (type (B)).

The resonator consists of two transmission lines of different characteristic impedances Z_1 and Z_2, of admittance Y_1 and Y_2, and corresponding length l_1 and l_2. The parameter K is defined by the impedance ratio Z_2/Z_1. The case of $K=1$ corresponds to UIR, so UIR can be considered for a special case of SIR.

For the admittance of the resonator from the open end, Y_i is given by

$$Y_i = jY_2 \frac{Y_2 \tan\beta l_1 \cdot \tan\beta l_2 - Y_1}{Y_2 \tan\beta l_1 + Y_1 \tan\beta l_2}. \tag{1}$$

The resonance condition can be described by

$$\tan\beta l_1 \cdot \tan\beta l_2 = Y_1/Y_2 = Z_2/Z_1 \equiv K \tag{2}$$

where

$$\beta = \sqrt{\epsilon_r} \cdot 2\pi/\lambda_0$$

$$Z_1 = 1/Y_1 = 60\ln(b_1/a_1)/\sqrt{\epsilon_r}$$

$$Z_2 = 1/Y_2 = 60\ln(b_1/a_2)/\sqrt{\epsilon_r}, \quad \text{type (A) structure}$$

$$60\ln(b_2/a_1)/\sqrt{\epsilon_r}, \quad \text{type (B) structure}$$

ϵ_r relative dielectric constant of material,
λ_0 wavelength in free space.

The resonator length l_t can be obtained from (2) as

$$l_t = l_1 + l_2 = l_1 + \frac{1}{\beta}\tan^{-1}\left(\frac{K}{\tan\beta l_1}\right). \tag{3}$$

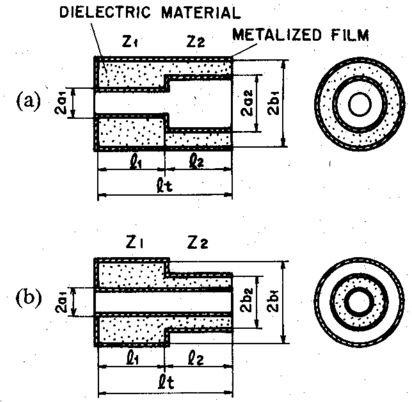

Fig. 1. Structures of the SIR. (a) Type (A) structure. (b) Type (B) structure.

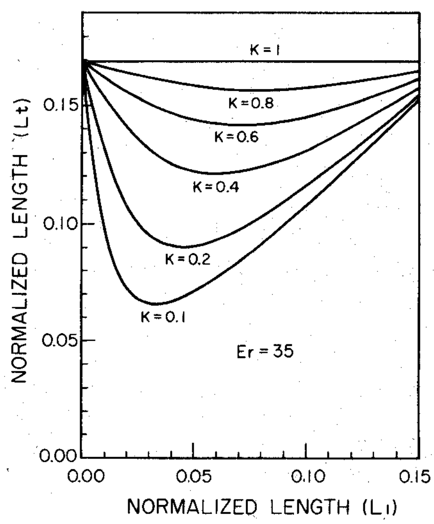

Fig. 2. Resonance condition of the SIR.

The result calculated for the relative dielectric constant $\epsilon_r = 35$ is shown in Fig. 2. L_1, L_t shown in Fig. 2 are l_1, l_t normalized by quarter-wavelength in free space, respectively. The region of $K=1$ and the region of $0<K<1$ indicate the resonance of the UIR and that of the SIR, respectively. In the region of $0<K<1$, the resonator has a minimum length at $l_1 = l_2 = \tan^{-1}\sqrt{K}/\beta$. Thus, the minimum resonator length $l_t \min$ can be obtained as follows:

$$l_t \min = 2\tan^{-1}\sqrt{K}/\beta. \tag{4}$$

In this way, the design equation becomes simple and practical when the lengths of Z_1 and Z_2 are equal.

The spurious response of the resonator is one of the important design factors. In particular, the output filters of nonlinear circuits such as oscillators and amplifiers should have the ability to provide harmonics suppression.

The UIR's have spurious responses in the odd-numbered times of the fundamental frequency, so the harmonics suppression cannot be expected. However, the SIR's possess this harmonics suppression characteristics.

When the lengths of Z_1 and Z_2 are equal, the resonance condition can be obtained from (2)

$$\tan^2 n\beta l = K. \tag{5}$$

When $n=1$, this equation shows the fundamental resonance condition. When $n>1$, it shows the spurious resonance condition.

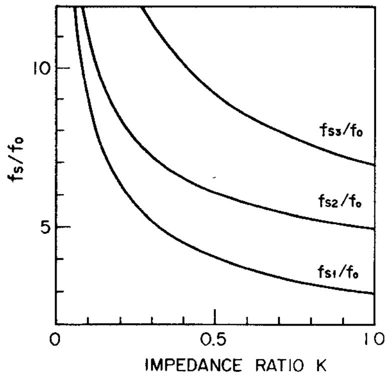

Fig. 3. Spurious resonance frequencies of the SIR.

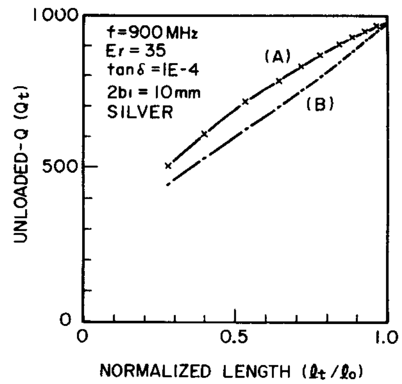

Fig. 4. Unloaded-Q as a function of the normalized resonator length.

The spurious resonance frequencies are defined by $f_{sn}(n = 1,2,\cdots)$

$$\left.\begin{aligned} f_{s1} &= \left(\frac{\pi}{\tan^{-1}\sqrt{K}} - 1\right) f_0 \\ f_{s2} &= f_{s1} + 2f_0 \\ f_{s3} &= 2f_{s1} + f_0 \end{aligned}\right\}. \tag{6}$$

In this way, the spurious resonance frequency can be controlled by the impedance ratio K.

Fig. 3 indicates the spurious resonance frequencies of the SIR as a function of the impedance ratio K.

B. Unloaded-Q

The unloaded-Q is an important parameter to determine the diameter of a coaxial resonator. The unloaded-Q, Q_0 of the dielectric-filled SIR, can be obtained by solving the electromagnetic field of the TEM mode

$$Q_0 = \frac{Q_c}{1 + Q_c \tan d} \tag{7}$$

where $\tan d$ is the loss tangent of the dielectric material, and where, for the type (A) structure

$$Q_c = \frac{2b_1}{\delta} \frac{A_1 \ln(b_1/a_1) + A_2 B_2 \ln(b_1/a_2)}{\left[A_1\{1+(b_1/a_1)\} + A_2 B_2\{1+(b_1/a_2)\} + \left(8\pi\sqrt{\epsilon_r}\, b_1/\lambda_0\right)\{\ln(b_1/a_1) + B_1 \ln(a_2/a_1)\}\right]}.$$

For the type (B) structure

$$Q_c = \frac{2b_1}{\delta} \frac{A_1 \ln(b_1/a_1) + A_2 B_2 \ln(b_2/a_1)}{\left[A_1\{1+(b_1/a_1)\} + A_2 B_2\{(b_1/b_2)+(b_1/a_1)\} + \left(8\pi\sqrt{\epsilon_r}\, b_1/\lambda_0\right)\{\ln(b_1/a_1) + B_1 \ln(b_1/b_2)\}\right]}$$

where δ is the skin depth, $A_1 = 2\beta l_1 + \sin 2\beta l_1$, $A_2 = 2\beta l_2 - \sin 2\beta l_2, B_1 = \cos^2 \beta l_1$, and $B_2 = \cos^2 \beta l_1 / \sin^2 \beta l_2$.

Usually, the impedance ratio K is set at less than unity to miniaturize the resonator length, so the outer radius b_1 becomes larger than b_2. When K and b_1 are constant, the type (A) SIR is more excellent, so that the unloaded-Q of the type (A) SIR is higher than that of the type (B) SIR.

As a calculation example, Fig. 4 shows the unloaded-Q as a function of the resonator length normalized by the dielectric-filled UIR.

Fig. 5 shows the unloaded-Q as a function of the outer diameter.

In the case of the dielectric-filled UIR, the unloaded-Q can be obtained by taking $K = 1$ and $l_1 = l_2$ in (7).

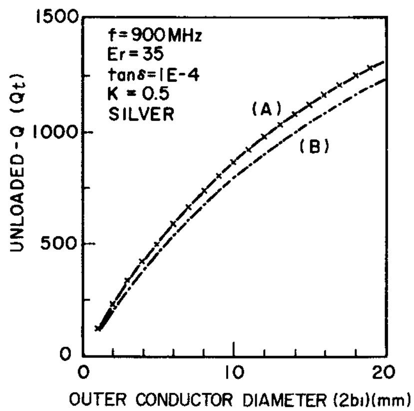

Fig. 5. Unloaded-Q as a function of the outer conductor diameter.

C. Admittance Slope Parameter

To design bandpass filters, the slope parameter b should be determined.

Calculated from its definition [4], the admittance slope parameter can be obtained as follows:

$$\begin{aligned} b &= \frac{\theta_{01} Y_2}{2} \left\{ \frac{l_2}{l_1} + \frac{K(1+\tan^2\theta_{01})}{K^2 + \tan^2\theta_{01}} \right\} \\ &= \frac{\theta_{01} Y_2}{2} \left\{ \frac{l_2}{l_1} + \frac{K}{K^2 + (1-K^2)\sin^2\theta_{01}} \right\} \end{aligned} \tag{8}$$

where $\theta_{01} = \beta l_1 | \omega = \omega_0$.

When $l_1 = l_2$, the condition of the minimum resonator length, the admittance slope parameter is simplified as follows:

$$b = \frac{\theta_{01} Y_2}{2} \cdot 2 = \theta_{01} Y_2. \tag{9}$$

III. Design of a Capacitively Coupled Bandpass Filter

The fundamental configuration of an n-stage capacitively coupled bandpass filter is shown in Fig. 6. G_A and G_B indicate input and output conductance, respectively, b_j indicates the admittance slope parameter of the jth resonator, and $C_{j,j+1}$ indicates coupling capacitance.

When the element values of the low-pass filter prototype g_j and the relative bandwidth w are given as fundamental design parameters of the bandpass filter, the admittance inverter param-

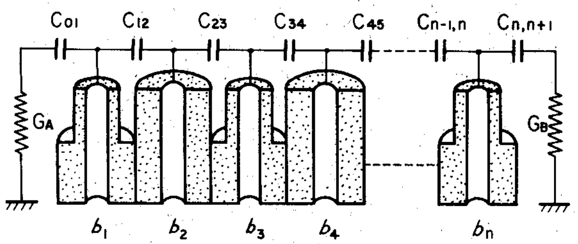

Fig. 6. Configuration of an n-stage capacitively coupled bandpass filter.

eter $J_{j,j+1}$ can be expressed as

$$\left.\begin{aligned} J_{01} &= \sqrt{\frac{G_A b_1 w}{g_0 g_1}} \\ J_{j,j+1} &= w\sqrt{\frac{b_j b_{j+1}}{g_j g_{j+1}}}\quad (j=1 \sim n-1) \\ J_{n,n+1} &= \sqrt{\frac{G_B b_n w}{g_n g_{n+1}}} \end{aligned}\right\}. \qquad (10)$$

Using these admittance inverter parameters, the coupling capacitance is given as follows:

$$\left.\begin{aligned} C_{01} &= \frac{J_{01}}{\omega_0\sqrt{1-(J_{01}/G_A)^2}} \\ C_{j,j+1} &= \frac{J_{j,j+1}}{\omega_0}(j=1 \sim n-1) \\ C_{n,n+1} &= \frac{J_{n,n+1}}{\omega_0\sqrt{1-(J_{n,n+1}/G_B)^2}} \end{aligned}\right\}. \qquad (11)$$

As the resonator size can be calculated using the results obtained in the previous section, it is possible to design a capacitively coupled bandpass filter with arbitrarily structured resonators.

IV. Consideration for Spurious Suppression

A. The Method for Spurious Suppression

Output filters of nonlinear circuits such as oscillators and amplifiers should have the ability to provide wide stopband characteristics for harmonics suppression.

For capacitively coupled filters using dielectric-filled coaxial resonators, the design method which combines differently structured resonators is effective to ensure wide stopband characteristics. The basis of this method is the use of different types of resonators with the same fundamental resonance frequencies but with different spurious resonance frequencies. The degree of spurious suppression depends upon the number of resonators and the span between the spurious frequencies of each resonator. The more resonators and the wider span between resonators, the more spurious suppression can be realized.

As an example, a bandpass filter combining UIR's with SIR's will be discussed. As described in the previous section, UIR's have spurious responses in the odd-numbered times of the fundamental frequency, while SIR's have spurious responses controlled by the impedance ratio K.

Now consider the case which suppresses the spurious response to five times the fundamental frequency.

Referring to Fig. 3, the selection of the impedance ratio K should be less than $K = 0.2$ or near $K = 0.5$. For consideration of the unloaded-Q of the resonator, it is desirable to set near $K = 0.5$.

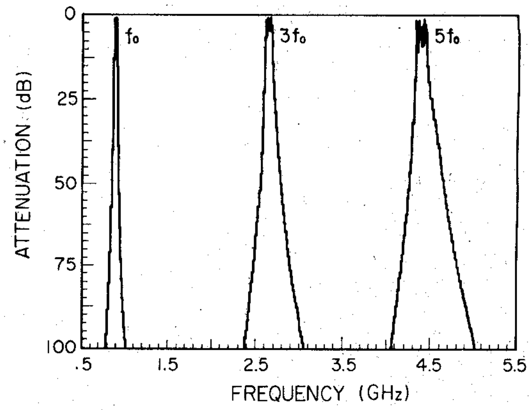

Fig. 7. Calculated spurious response of the bandpass filter using UIR's.

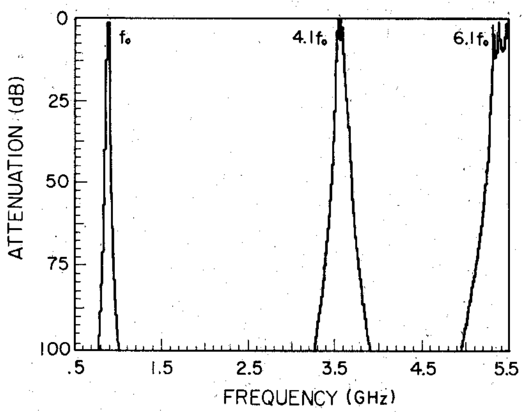

Fig. 8. Calculated spurious response of the bandpass filter using SIR's.

B. Computer Simulation of the Stopband Characteristics

Fundamental design parameters of the bandpass filter using computer simulation are as follows:

Center Frequency:	$f = 877.5$ MHz
Number of Resonators:	$N = 5$
Filter Response:	Chebyshev type
Passband Ripple:	$R = 0.02$ dB
Relative Bandwidth:	$w = 0.03$
Unloaded-Q (UIR):	900
(SIR):	850.

Firstly, consider that the bandpass filter consists of the same resonators. Figs. 7 and 8 show the response of the bandpass filter consisting of UIR's and SIR's ($K = 0.5$), respectively. The bandpass filter consisting of the same resonators has a spurious response corresponding to the impedance ratio K, so the stopband characteristics of the bandpass filter are not satisfied. However, spurious frequencies of the bandpass filter consisting of SIR's ($K = 0.5$) are 4.1 and 6.1 times, respectively, the fundamental frequency. These spurious frequencies are different from the odd times of the fundamental frequency, so this bandpass filter has the ability to suppress the harmonics in oscillators or amplifiers.

Secondly, consider the bandpass filter consisting of different resonators, UIR's and SIR's. In this bandpass filter, UIR's and SIR's will not be resonant at the spurious frequency of SIR's and that of UIR's, respectively. Thus, to obtain wide stopband char-

TABLE I
CALCULATED SPURIOUS RESPONSE OF THE BANDPASS FILTER USING UIR'S AND SIR'S.

No	Combination of Resonators	Spurious response $3f_0$	$4.1f_0$	$5f_0$	$6.1f_0$
I	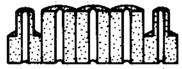	−44 dB	<−100dB	−35dB	<−100dB
II		−51	−31	−77	−15
III	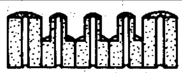	<−100	−21	<−100	−24
IV		−47	−61	−51	−69

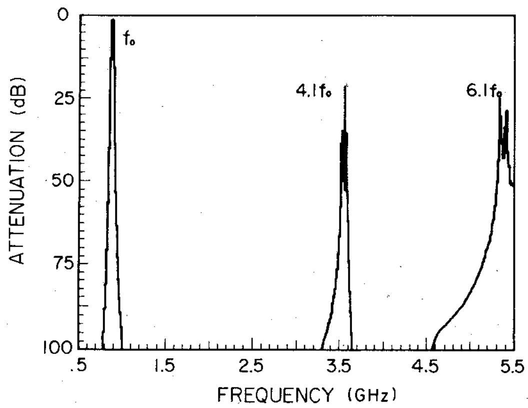

Fig. 9. Calculated spurious response of the bandpass filter using UIR's and SIR's (No. III).

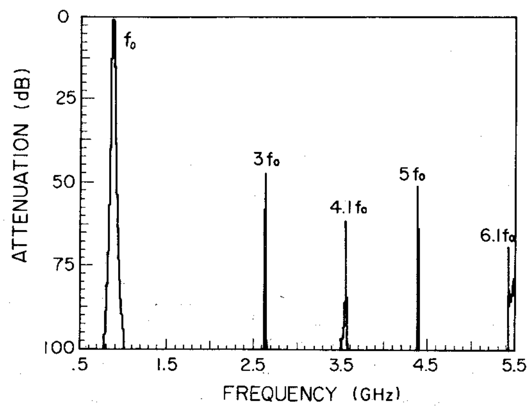

Fig. 10. Calculated spurious response of the bandpass filter using UIR's and SIR's (No. IV).

acteristics, it is desirable to choose a similar stage number of UIR's and SIR's in the filter.

Some results of computer simulation for the bandpass filter using both UIR's and SIR's are summarized in Table I. Figs. 9 and 10 show the spurious response of Nos. III and IV combinations, respectively. The No. III combination has the response which makes the spurious response of the SIR remarkable, and only a 21-dB spurious suppression can be obtained. The No. IV combination has all the spurious responses of UIR's and SIR's, but these spurious responses can be eliminated as mentioned before, and a computer simulation made it clear that more than

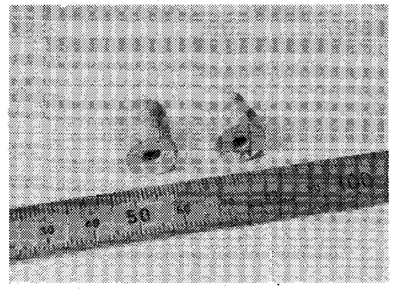

Fig. 11. Photograph of the dielectric-filled coaxial UIR (left) and SIR (right).

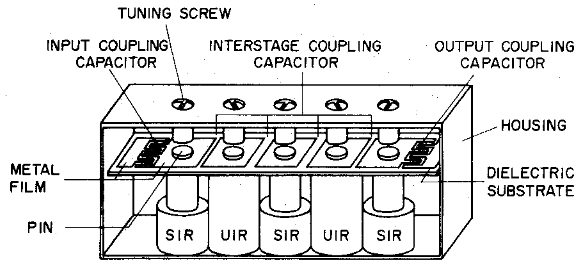

Fig. 12. Longitudinal cutaway of the fabricated bandpass filter.

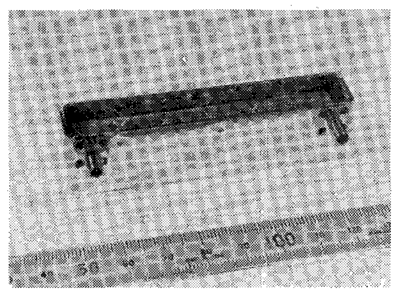

Fig. 13. Photograph of the fabricated bandpass filter.

45-dB spurious suppression can be achieved, as shown in Fig. 10. This is one of the combinations which show excellent wide stopband characteristics.

According to the above analysis, we selected the No. IV combination in the design example.

V. FABRICATION AND PERFORMANCE OF AN EXPERIMENTAL FILTER

On the basis of the previous results, an experimental bandpass filter was designed and fabricated. The five-stage bandpass filter fabricated here consists of dielectric-filled coaxial UIR's and SIR's as shown in Fig. 11. To obtain the unloaded-Q estimated in the previous simulation, resonators have inner and outer diameters of 4 mm and 12 mm, respectively. The stepped outer diameter is 7 mm for an impedance ratio $K = 0.5$. The unloaded-Q of the type (A) SIR is higher than that of the type (B) SIR, but the type (B) SIR is used because it is simple to fabricate. The relative dielectric constant of this material is 35 and its loss tangent is less than 1×10^{-4} at 12 GHz [5].

Fig. 12 shows a longitudinal cutaway of the fabricated filter. The coupling capacitor was fabricated on a dielectric substrate with a relative dielectric constant of 2.5 and a loss tangent of 2×10^{-3}. Interdigital capacitors and gap capacitors were introduced for input (output) couplings and interstage couplings between resonators, respectively. The structure of capacitors was determined by experimental results of the external-Q and coupling factor. For alignment and adjustment of the fabricated

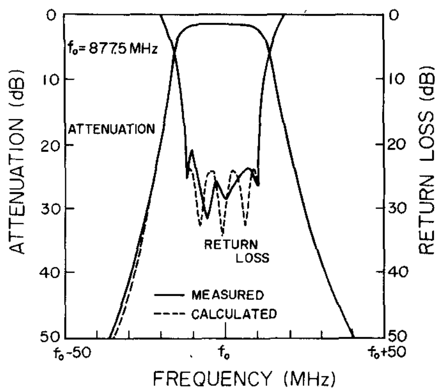

Fig. 14. Measured and calculated frequency response of the experimental bandpass filter.

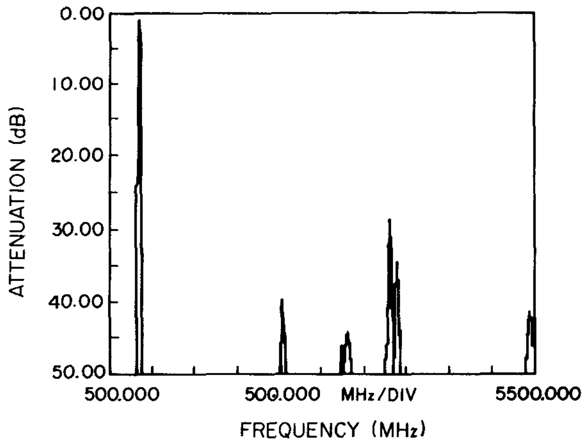

Fig. 15. Measured spurious response of the fabricated bandpass filter.

filter, it was necessary to tune resonators with tuning screws, but no adjustment of coupling capacitors was required, so coupling capacitors were precisely determined by photolithographic technology.

Fig. 13 shows the outer view of the fabricated filter. Its physical dimensions are 80 mm (length)×14 mm (width)×20 mm (height) and its volume is 22.4 cm^3.

Fig. 14 shows the measured and calculated frequency response of the experimental bandpass filter. The solid and dotted lines indicate the measured and calculated responses, respectively. The fabricated filter performance shows close coincidence with the design results. Therefore, the propriety of the design formulas is experimentally verified. Passband insertion loss was obtained at 1.6 dB at midband and 1.85 dB at band edge.

Fig. 15 shows the measured spurious response. It is similar to the spurious response of the computer simulation. But the spurious response near 3.8 GHz doesn't appear in the simulation. The spurious response near 3.8 GHz is different from that of the TEM mode in a coaxial resonator, UIR, and SIR. Consideration concerning spurious frequency and the diameter of the resonator proved this unknown mode to be a TE_{21} mode.

VI. Conclusions

A method of designing capacitively coupled bandpass filters with arbitrarily structured resonators was established and the fabricated filter performance showed close coincidence with the design results. It is shown that wide stopband characteristics can be realized by combining quarter-wavelength uniform impedance resonators (UIR's) with stepped impedance resonators (SIR's). The special feature of this filter is that the spurious response can be controlled by the impedance ratio K of the SIR and the combination of UIR's and SIR's.

Acknowledgment

The authors wish to thank Dr. S. Kisaka for his continuous encouragement and Dr. H. Ouchi and S. Kawashima for developing the materials. Thanks are also due to K. Eguchi and K. Kikuchi for their experimental work.

References

[1] M. Makimoto and S. Yamashita, "Compact bandpass filters using stepped impedance resonators," *Proc. IEEE*, vol. 67, pp. 16–19, Jan. 1979.

[2] M. Makimoto and S. Yamashita, "Bandpass filters using parallel coupled strip-line stepped impedance resonators," in *IEEE MTT-S Int. Microwave Symp.*, May 1980, pp. 141–143.

[3] S. Yamashita and M. Makimoto, "Miniaturized coaxial resonator partially loaded with high-dielectric-constant microwave ceramics," *IEEE Trans. Microwave Theory Tech.*, vol. MTT-31, pp. 697–703, Sept. 1983.

[4] G. L. Matthaei, L. Young, and E. M. T. Jones, *Microwave Filters, Impedance-Matching Networks, and Coupling Structures.* New York: McGraw-Hill, 1964.

[5] S. Kawashima *et al.*, "Dielectric properties of $Ba(Zn_{1/3}Nb_{2/3})O_3$-$Ba(Zn_{1/3}Ta_{2/3})O_3$ ceramics at microwave frequency," in *Proc. First Meeting on Ferroelectric and Their Applications*, Apr. 1978, pp. 293–296.

Conservation Laws for Distributed Four-Ports

O. SCHWELB, MEMBER, IEEE, AND R. ANTEPYAN, STUDENT MEMBER, IEEE

***Abstract*—Condition of reciprocity, losslessness, bilateral symmetry, transversal symmetry, and semireciprocity is given for a four-port in terms of its impedance, admittance, scattering, and transfer representation. Corresponding conditions are also presented for the system coupling matrix of a uniform distributed circuit. The results are applied to an anisotropic stratified waveguide.**

I. Introduction

Classical network analysis has provided invaluable analytical tools for the design of microwave devices. Circuit methods, however, are far less prevalent in integrated optics, acoustooptics, and related areas. The purpose of this paper is to provide, in tabular form, conditions for certain properties of integrated circuits. These properties include reciprocity, losslessness, bilateral and transversal symmetry, and semireciprocity. The last one of these, exhibited by anisotropic media, appears to be novel.

The conservation laws are expressed in terms of various, commonly used terminal representations, such as impedance, admittance, scattering, scattering transfer, etc., as well as in terms of the system coupling matrix of a uniform distributed network. Conversion from one representation to another is facilitated by a computer program developed by one of the authors (RA). The

Manuscript received February 17, 1984; revised August 13, 1984. This work was supported in part by the Natural Sciences and Engineering Research Council, Canada, and by the FCAC, Quebec.

The authors are with the Department of Electrical Engineering, Concordia University, Montreal, Quebec, Canada H3G 1M8.

0018-9480/85/0002-0157$01.00 ©1985 IEEE